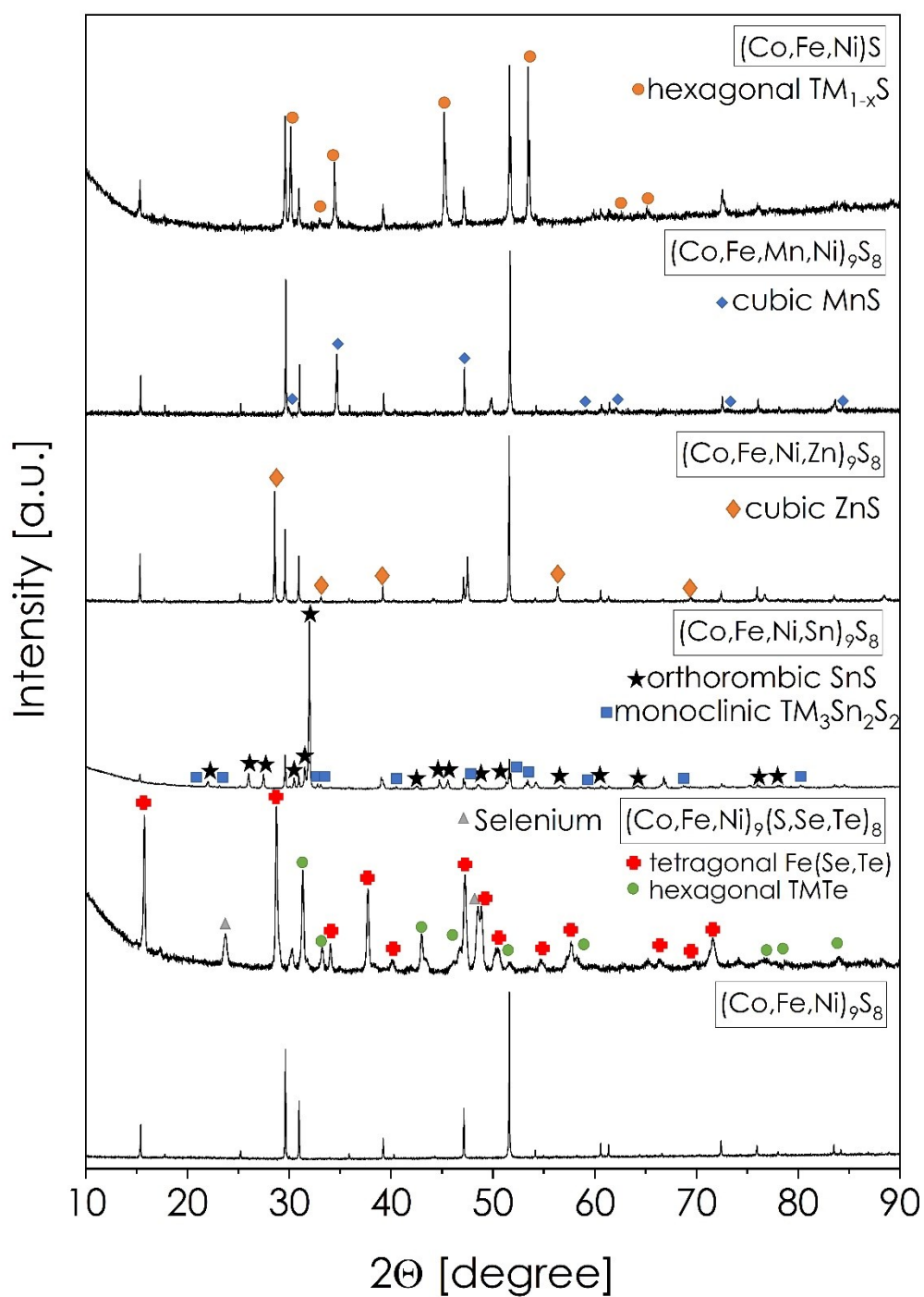
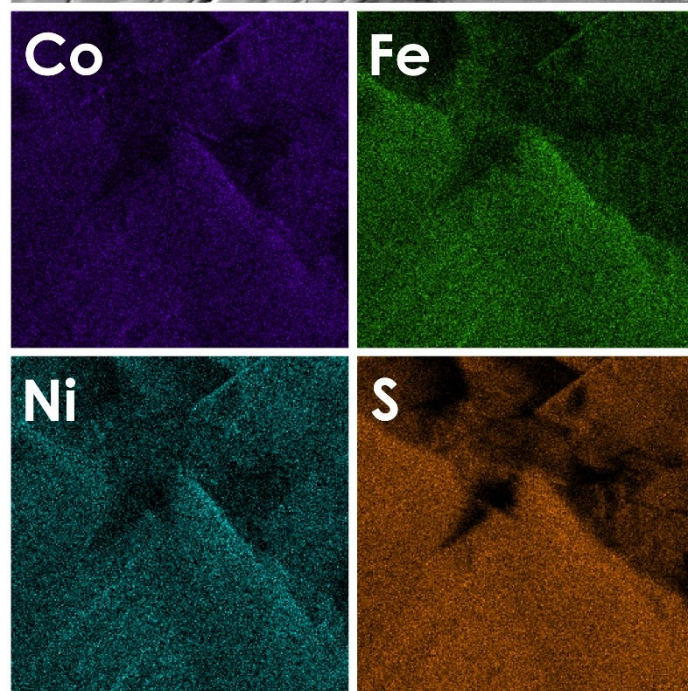
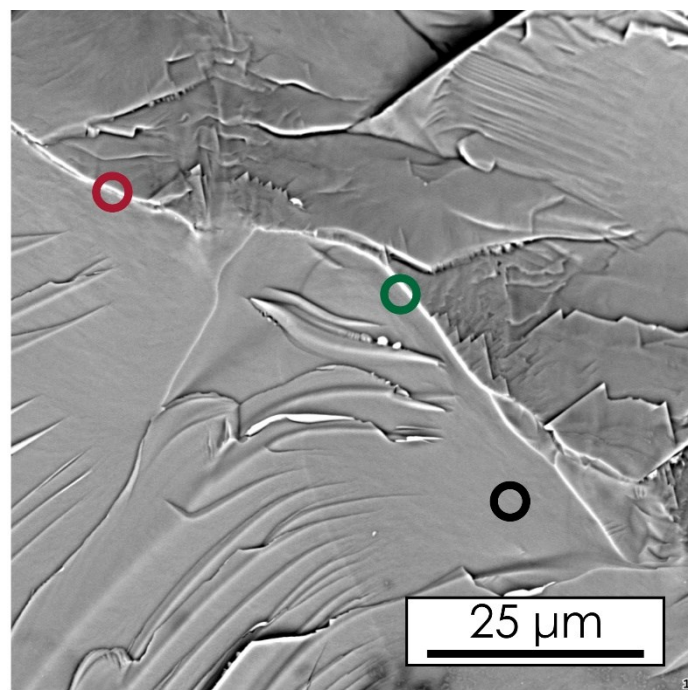


**SI.Fig. 1.** Thermal diffusivity and specific heat ( $\text{Cp}$ ) measurements for  $\text{TM}_9\text{S}_8$  (a) and  $\text{TM}_9\text{Ch}_8$  IHP-sintered pellets.



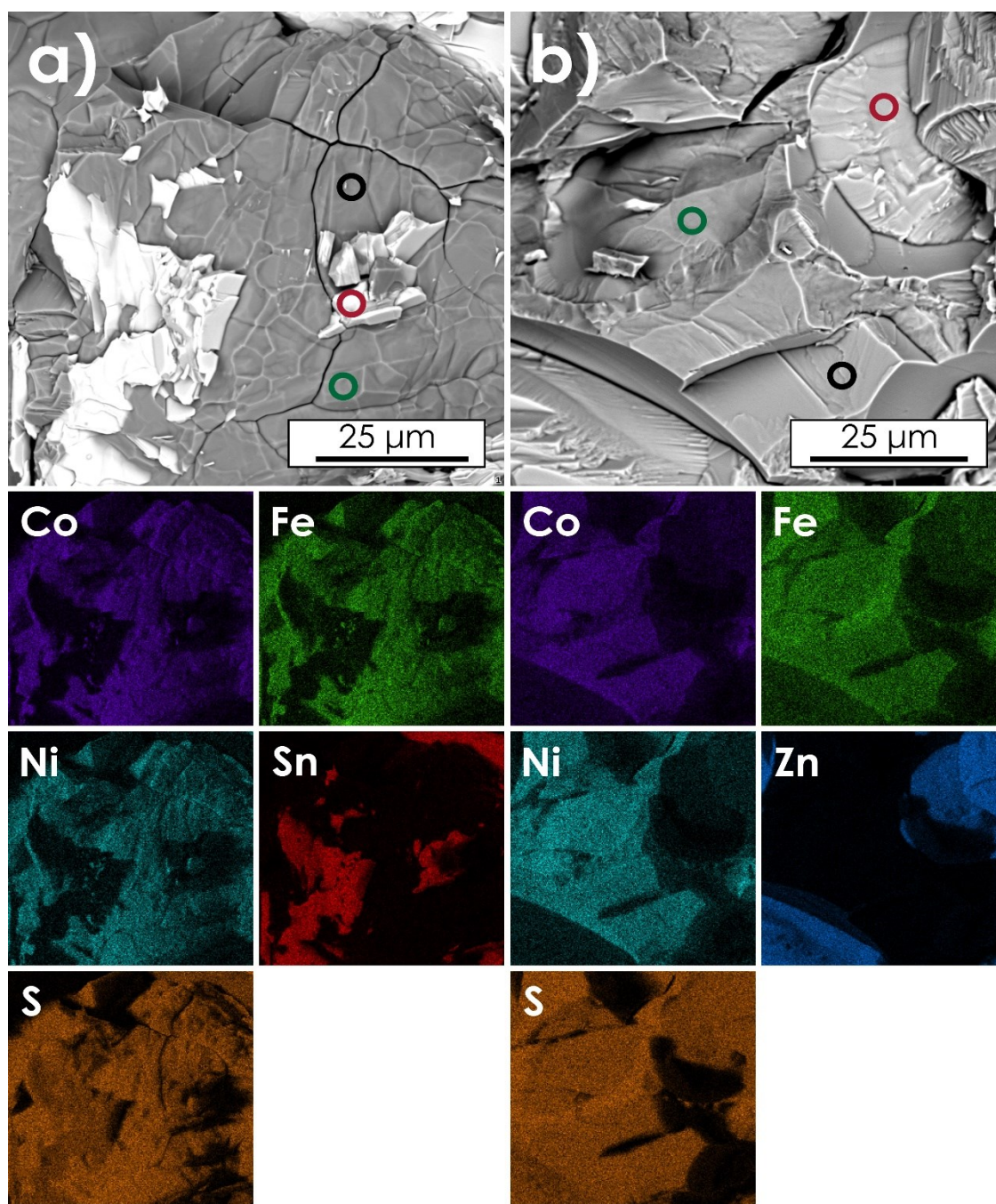
**SI.Fig. 2.** XRD diffraction patterns of the multi-phase  $(\text{Co,Fe,Ni})\text{S}$ ,  $(\text{Co,Fe,Mn,Ni})_9\text{S}_8$ ,  $(\text{Co,Fe,Ni,Sn})_9\text{S}_8$ ,  $(\text{Co,Fe,Ni,Zn})_9\text{S}_8$ ,  $(\text{Co,Fe,Ni})_9(\text{S,Se,Te})_8$ , and single-phase  $(\text{Co,Fe,Ni})_9\text{S}_8$  pentlandite powder samples.



	Co	Fe	Ni	S
avg	22.6	19,4	17.3	40.8
○	14.3	22.2	15.8	47.7
○	14.0	22.2	12.8	51.1
○	17.9	19.9	14.6	47.6

**SI.Fig. 3.** SEM micrographs together with the corresponding EDS mappings and point/area analysis. All data was collected from the fractured, as-synthesized (Co,Fe,Ni)S ingot.





	Co	Fe	Ni	Sn	S		Co	Fe	Ni	Zn	S
avg	21.3	13.4	16.2	11.4	37.8	avg	14.5	13.8	16.0	12.7	43.0
⊙	2.6	1.6	1.8	54.1	39.9	⊙	6.3	7.6	1.3	36.1	48.7
⊙	23.1	14.1	18.3	0.1	44.4	⊙	17.9	12.3	23.4	0.0	46.4
⊙	24.6	14.3	19.3	0.9	41.0	⊙	19.2	11.0	22.9	0.0	46.9

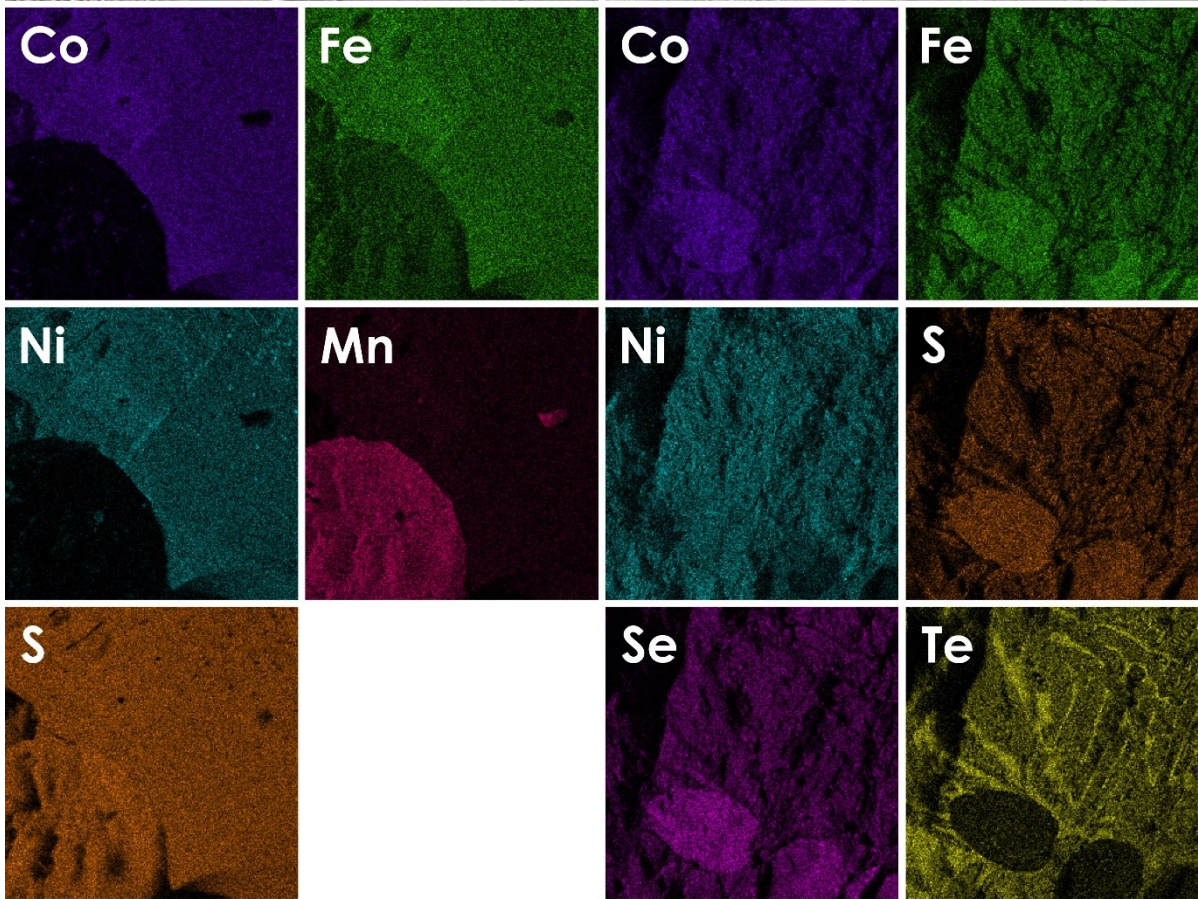
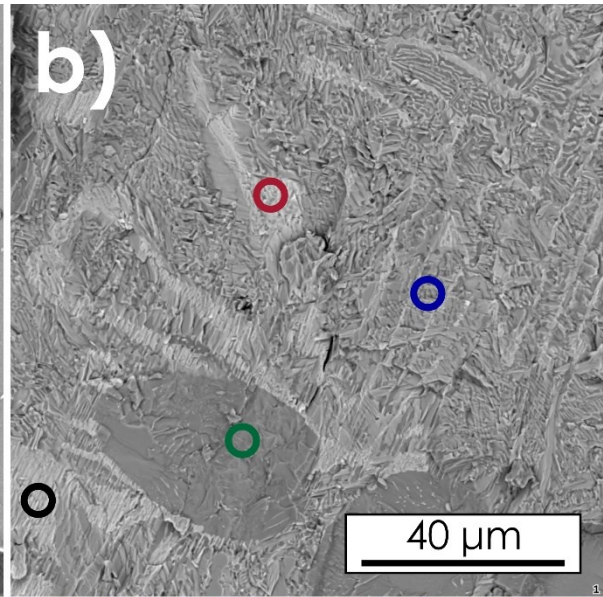
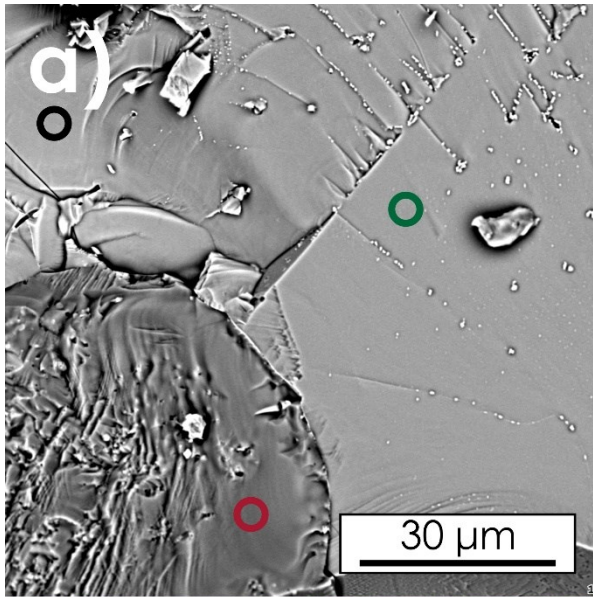
SI.Fig

4. SEM micrographs together with the corresponding EDS mappings and point/area analysis.

All data was collected from the fractured, as-synthesized  $(\text{Co,Fe,Ni,Sn})_9\text{S}_8$  (a), and

$(\text{Co,Fe,Ni,Zn})_9\text{S}_8$  ingots.





	Co	Fe	Ni	Mn	S		Co	Fe	Ni	S	Se	Te
avg	16.8	17.9	17.1	24.0	23.5	avg	18.0	16.3	16.4	12.4	19.4	17.6
○	1.6	19.1	0.1	44.7	34.6	○	18.7	3.3	26.8	1.1	2.5	47.6
○	21.9	14.9	18.7	0.1	44.4	○	21.9	15.0	11.1	21.3	27.9	2.9
○	21.0	14.9	18.3	0.5	45.3	○	15.3	7.1	22.5	4.0	10.4	40.7
						○	16.9	19.2	23.5	8.3	12.0	20.1

**SI.Fig. 5.** SEM micrographs together with the corresponding EDS mappings and point/area analysis. All data was collected from the fractured, as-synthesized  $(\text{Co,Fe,Mn,Ni})_9\text{S}_8$  (a), and  $(\text{Co,Fe,Ni})_9(\text{S,Se,Te})_8$  ingots.

**SI. Table 1 Structural data of the  $\text{TM}_9\text{S}_8$  pentlandites,**

Wyckoff position	$\text{TM}_9\text{S}_8$ powder		$\text{TM}_9\text{S}_8$ pellet	
	Occupancy	B iso	Occupancy	B iso
4a	Co – 0.42, Fe – 0.28, Ni – 0.36	Co – 0.50, Fe – 0.50, Ni – 0.50	Co – 0.42, Fe – 0.26, Ni – 0.32	Co – 0.50, Fe – 0.50, Ni – 0.50
32f	Co – 0.42, Fe – 0.28, Ni – 0.36	Co – 0.50, Fe – 0.5, Ni – 0.5	Co – 0.42, Fe – 0.26, Ni – 0.32	Co – 0.50, Fe – 0.5, Ni – 0.50
8c	S – 1.0	S – 1.15	S – 1.0	S – 1.15
24e	S – 1.0	S – 0.50	S – 1.0	S – 0.50

**SI. Table 2 Structural data of the  $\text{TM}_9\text{Ch}_8$  pentlandites.**

Wyckoff position	$\text{TM}_9\text{Ch}_8$ powder		$\text{TM}_9\text{Ch}_8$ pellet	
	Occupancy	B iso	Occupancy	B iso
4a	Co – 0.30, Fe – 0.34, Ni – 0.36	Co – 1.21, Fe – 1.27, Ni – 1.27	Co – 0.30, Fe – 0.34, Ni – 0.36	Co – 1.21, Fe – 1.27, Ni – 1.27
32f	Co – 0.30, Fe – 0.34, Ni – 0.36	Co – 1.21, Fe – 1.27, Ni – 1.27	Co – 0.30, Fe – 0.34, Ni – 0.36	Co – 1.21, Fe – 1.27, Ni – 1.27
8c	S – 0.50, Se – 0.50	S – 0.78, Se – 0.40	S – 0.44, Se – 0.56	S – 0.78, Se – 0.50
24e	S – 0.50, Se – 0.50	S – 0.78, Se – 0.40	S – 0.60, Se – 0.40	S – 0.78, Se – 0.45